COS Instrument Science Report 2010-03(v1)

COS Near-UV Flat Fields and High S/N Determination from SMOV Data

Thomas B. Ake[1], Eric B. Burgh[2], and Steven V. Penton[2]

[1] Space Telescope Science Institute, Baltimore, MD
[2] Center for Astrophysics and Space Astronomy, University of Colorado - Boulder

04 February 2010

ABSTRACT

We describe the data taken with the internal flat-field lamp during the Servicing Mission Observatory Verification (SMOV) phase of COS to produce a high-quality near-UV (NUV) flat-field image. These data were compared to the flat-field image created during thermal-vacuum (TV) testing to examine the latter's applicability for pipeline processing. The alignment between the on-orbit and ground flats is estimated to be better than one pixel, allowing the SMOV and TV data to be combined into a superflat reference file. This file also was updated to include a vignetting correction needed for external observations. We show that the use of flat fielding and FP-POS splitting can produce spectra with signal-to-noise greater than 100:1 in all NUV spectroscopic modes.

Contents:

1. Introduction and Overview

The Cosmic Origins Spectrograph (COS) was installed on *HST* in the axial instrument bay occupied by COSTAR during Servicing Mission 4 (SM4), in May 2009. The near-UV (NUV) channel of COS consists of four first-order gratings for spectroscopy and a mirror for target acquisition and imaging (Soderblom et al. 2007). The light from these is imaged onto a CsTe MAMA detector by three camera mirrors (NCM3 a,b,c), resulting in non-contiguous pieces of a first order spectrum being stacked into three stripes on the two-dimensional detector. The instrument contains a flat-field calibration system to allow the removal of small-scale detector structures during processing of the science data (COS OP-01). It consists of two redundant deuterium lamps and a flat-field calibration aperture (FCA). Light from a lamp enters the spectrograph through the FCA such that it follows nearly the same optical path as an external target, reflecting off the gratings and other optical elements before striking the detector. Thus the lamp only illuminates the area on the detector where external science data are present. In particular, the location where wavelength calibration spectra occur is not flat fielded.

This ISR describes the development of the flat-field reference file for the NUV channel of COS for pipeline processing. It further characterizes the signal-to-noise (S/N) achievable in the various NUV spectroscopic modes.

2. Flat-Field Observations

2.1 Thermal-Vacuum Testing

The thermal-vacuum (TV) flat-field data comprise observations taken in 2003 and 2006 (COS AV-04). Exposures were obtained with both internal and external D2 calibration lamps. Internal observations are made with the FCA, which is wide enough to allow illumination across the full science area of the detector. The external data were taken through the primary science aperture (PSA), which was positioned at various cross-dispersion locations on the detector due to the narrower height of the source. The 2003 data include about 3.6 billion counts taken in ACCUM mode, accounting for about 98% of all the flat-field data, as well as 84 million counts in time-tagged mode. The 2006 data added an additional one million counts. Most of the counts going into the resultant TV ground flat came from the external lamp.

2.2 SMOV Internal Flat Observations (Program 11478)

SMOV program 11478 obtained a series of 1800-second exposures of one of the internal deuterium lamps, with twelve exposures at each of three central wavelengths of the G185M grating (1835, 1850 and 1864 Å). These were structured as thirty-six individual visits, with all the exposures at a particular wavelength setting being taken consecutively before changing to another wavelength. Each exposure produced between 6 and 10 counts per pixel (50-100 per 3x3 pixel resolution element) in the region covered by the FCA. All thirty six exposures were combined for a total of at least 200 counts per pixel (1800 counts per 3x3 pixel resolution element). Table 1 lists the data sets that were obtained.

Table 1 : NUV Flat Field Observations (SMOV 11478)

Rootname	Cenwave	Date-Obs	Time-Obs	Rootname	Cenwave	Date-Obs	Time-Obs
la8101eiq	1835	2009-07-21	06:46:46	la8119ddq	1850	2009-07-27	14:39:25
la8102x2q	1835	2009-07-23	07:36:08	la8120dlq	1850	2009-07-27	16:19:01
la8103xfq	1835	2009-07-23	08:19:56	la8121e2q	1850	2009-07-27	17:58:00
la8104ysq	1835	2009-07-23	09:44:56	la8122ebs	1850	2009-07-27	18:40:58
la8105aaq	1835	2009-07-23	11:28:36	la8123ehq	1850	2009-07-27	19:44:10
la8106bzq	1835	2009-07-23	13:19:56	la8124erq	1850	2009-07-27	20:35:46
la8107coq	1835	2009-07-23	16:30:33	la8125f4q	1864	2009-07-27	21:37:55
la8108g4q	1835	2009-07-23	21:26:48	la8126fcq	1864	2009-07-27	22:21:43
la8109g6q	1835	2009-07-23	22:20:07	la8127feq	1864	2009-07-27	23:05:31
la8110g8q	1835	2009-07-23	23:05:36	la8128fsq	1864	2009-07-28	00:05:36
la8111gkq	1835	2009-07-23	23:49:24	la8129fwq	1864	2009-07-28	00:56:24
la8112guq	1835	2009-07-24	00:33:12	la8130gbq	1864	2009-07-28	01:44:52
la8113gxq	1850	2009-07-24	01:17:36	la8131w6q	1864	2009-07-29	19:18:55
la8114h1q	1850	2009-07-24	02:00:09	la8132w2q	1864	2009-07-29	18:35:07
la8115h9q	1850	2009-07-24	02:42:42	la8133v9q	1864	2009-07-29	17:51:19
la8116hnq	1850	2009-07-24	03:34:15	la8134ttq	1864	2009-07-29	16:14:29
la8117hrq	1850	2009-07-24	04:28:00	la8135sxq	1864	2009-07-29	14:35:30
la8118i6q	1850	2009-07-24	05:33:29	la8136snq	1864	2009-07-29	13:14:01

The SMOV program was designed to repeat the internal observations taken during TV 2003 in time-tag mode. The initial step of the analysis plan was to evaluate whether the on-orbit flat made from these observations matched the ground flat from TV. If so, all the SMOV and TV data could be combined into a higher S/N flat for pipeline data processing; if not, further observations would be scheduled and a separate on-orbit flat would be created and used. The output of the lamps was expected to degrade with usage, so minimizing the number of exposures during SMOV would help preserve the lamps for checking flat-field changes later in the mission. Indeed, lamp output was reduced on the order of 25% after the roughly18 hours of usage for this program (Figure 1).

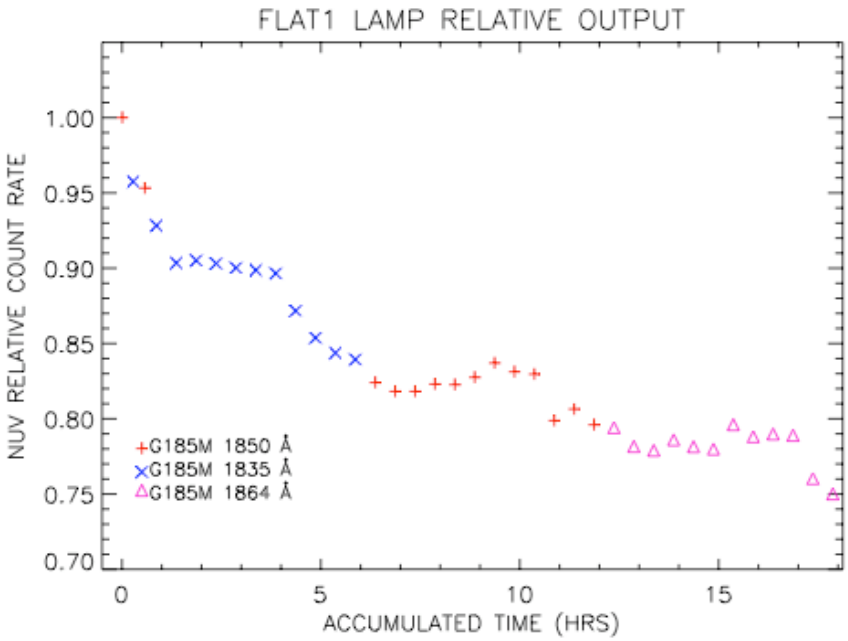

Figure 1: Degradation of the FLAT1 deuterium lamp output with accumulated exposure time. The lamp was used at the highest current setting. The initial measurement was a 60 sec exposure taken during the functional checkout after COS was installed into HST. Count rates for Cenwaves 1835 Å and 1864 Å were normalized to those of 1850 Å in their wavelength overlap regions to place them on the same relative scale.

The following section describes the construction of the on-orbit flat and its comparison with the TV flat field.

3. Flat-Field Creation and Comparison

As with other HST detectors, the intensity variations in the flat field can be considered to be the product of two components: the P-flat, which characterizes the small scale, pixel-to-pixel sensitivity fluctuations of the detector, and the L-flat, which accounts for low-frequency variations. In the CalCOS pipeline, a P-flat reference file is used to correct science data as one of the processing steps. The low-frequency variations are taken out by the sensitivity curves, which are created for each grating and central wavelength. To construct the flat-field reference file, an L-flat is derived from the D2 lamp data, including the spectrum of the lamp, the throughput of the optics, and any low-frequency detector variation. This is divided into the images to create the P-flat. In the wavelength region for the G185M grating, the lamps provide a continuous spectrum, simplifying the L-flat derivation. Since the L-flat is only needed to make the P-flat, it is discarded afterwards. The on-orbit and TV flat fields are the resulting P-flats from this process.

3.1 P-Flat Creation

For both the TV and on-orbit data, the flat fields were created as follows:

- Photon lists were concatenated for all time-tagged exposures.

- A 2-D image of counts as a function of X (along dispersion) and Y (cross-dispersion) was created from all the photon events.

- In the case of the TV ACCUM data, the images were co-added.

- Over the rows which define the science region on the detector, a row-by-row extraction was fitted by a 5th order polynomial to produce an L-Flat.

- The image was divided by the L-Flat to produce a P-Flat.

Three different methods of row-by-row extraction were performed and compared: a single row, the straight average of three rows, and a three-row weighted (i.e, half weight given to adjacent rows) extraction. In the end, the three methods had no discernable diference in the attainable signal-to-noise of flat-fielded data. The final product uses the simple row-by-row extraction.

3.2 Comparison between TV and SMOV Flats

The on-orbit flat was compared to the TV flat by several different means. First, the ground flat was divided into the on-orbit one, which would produce visible structures if the flat fields were not aligned. The ratio of the two images (Figure 2) produces a salt-and-pepper noise result, i.e., no significant fixed pattern structure in the division, indicating that the two flats match each other. A one pixel shift before taking the ratio produces a residual fringe pattern, indicating that the alignment between the two is within one pixel.

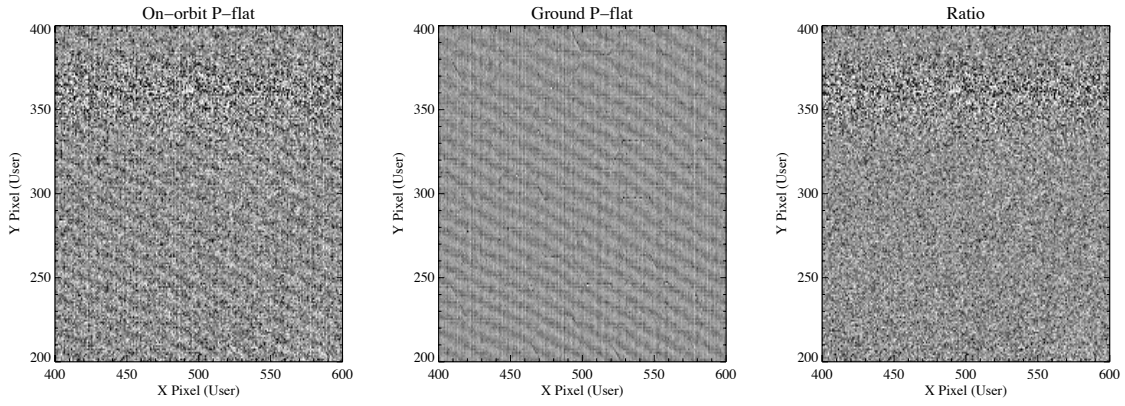

Figure 2: Comparison of a sub-region of the P-flats for the on-orbit and thermal-vaccum testing data.

Figure 3 shows a comparison of histograms of the flat-field values for the on-orbit flat, the ratio of the on-orbit to ground flat, as well as the result if there is a one pixel X-offset

between the two. The distribution of values in the ratio of the on-orbit flat by the ground flat has a narrower width and higher peak than the distribution of the values from the on-orbit flat alone. This indicates that the fixed-pattern noise has been reduced by the division of the on-orbit data by the ground flat. A distribution of the values from the ratio of a shifted version of the on-orbit flat by the ground flat has a broader distribution and lower peak, reflecting the systematic errors introduced by the shift.

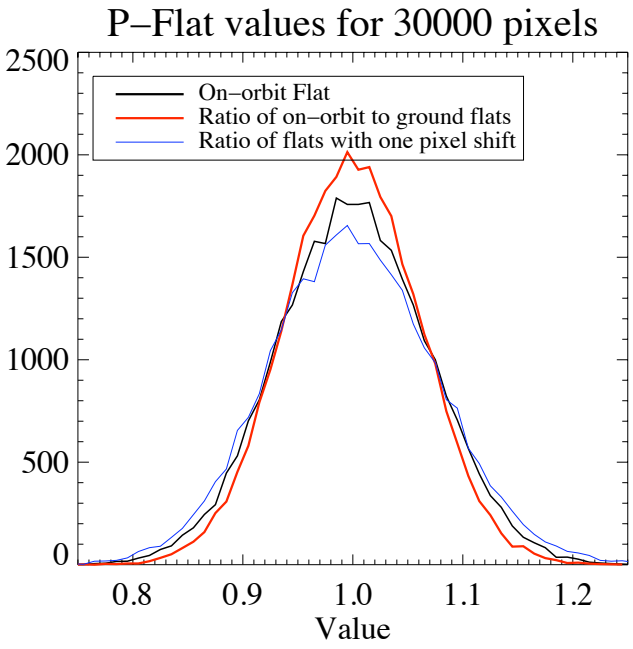

Figure 3: Comparison of the histograms of the flat-field values for the on-orbit flat, the ratio of the on-orbit to TV flat, as well as a one pixel offset between the two.

As a final check of the alignment of the detector format, the positions of detector blemishes in both flats were examined. As seen in Figure 4, the ground and on-orbit features are found at the same location, consistent with no format shift of the detector having occurred due to launch stresses.

Since the TV flat was found to match the SMOV one, all the ground and on-orbit data were combined and a superflat was created for pipeline processing. A Gaussian fit to the distribution of flat-field values yields $\sigma = 0.034$, indicating that the maximum S/N that can be obtained for a single exposure without flat fielding is ~ 30.

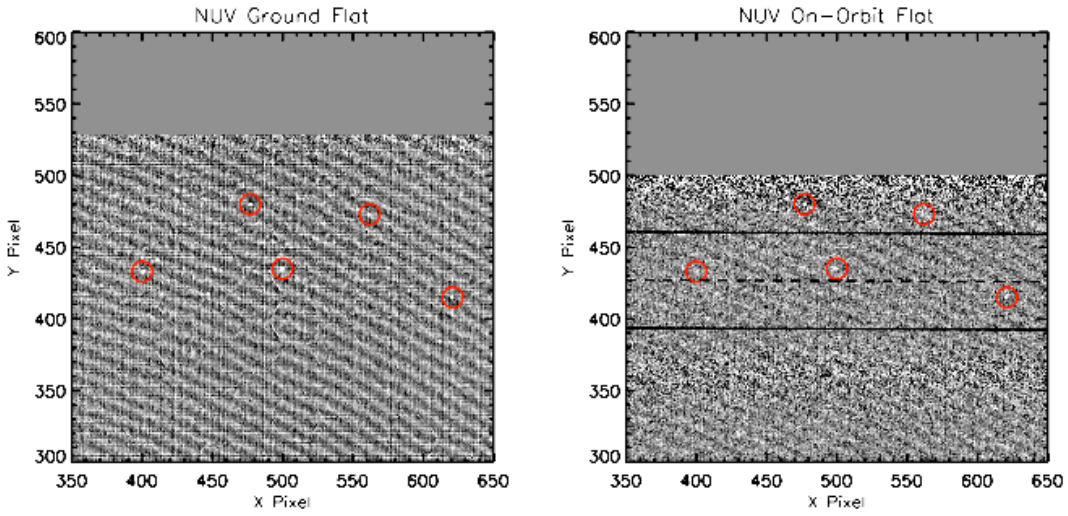

Figure 4: Locations of sample NUV blemishes in the ground (left) and on-orbit (right) flat fields. Red circles are centered at the same pixel positions for the two flats, illustrating that there is no shift in format between TV and SMOV. The horizontal lines indicate the edges and center of Stripe C on the detector.

4. Vignetting Correction

Durring SMOV, an unexpected result found in the observations of external targets was a depression in the counts at small X pixel values of the NUV channel (see left panel of Figure 5). This depression is not seen in the flat-field data taken through the FCA. All three PSA stripes are affected. The effect is consistent with ray-trace modeling where the optical beam partially misses the NCM3 camera mirrors. The beam from the D2 lamp is sufficiently different that this vignetting does not occur.

With the data obtained as part of the SMOV NUV high-S/N program (Section 5), the vignetting profile can be modeled. Three of the grating settings had long exposures, producing very high S/N spectra, allowing for the profile to be determined from nine different samplings (three stripes per setting). The difference between the FP-POS=1 and FP-POS=4 positions amounts to about a 150 pixel shift of the spectrum in the X direction on the detector. This is about the same number of pixels that are affected by the vignetting, so that a ratio of the two positions in wavelength space will produce the vignetting profile (see Figure 5). For each of the nine spectra, a ratio was measured and all nine averaged together. Since the shapes of the profiles were in agreement for the three stripes, all were combined. A fit was made to this profile with three variables: the maximum X location affected by the vignetting, the slope of the linear vignetting profile, and the number of pixels to smooth the function. Figure 6 shows the spectral ratio averaged for all nine spectra and the resultant best fit, with parameters of Maximum X = 162, slope = 0.00127, and smooth of 29 pixels.

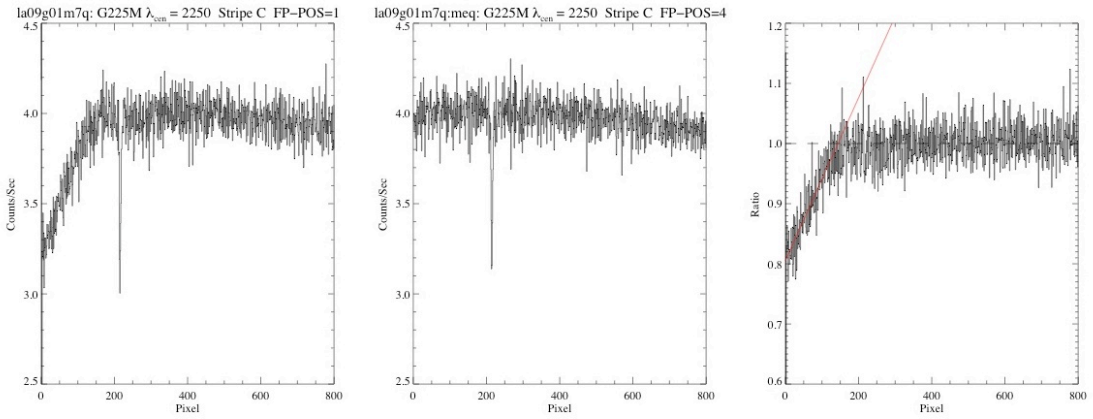

Figure 5: Spectra of G191-B2B showing the NUV vignetting at low X-pixel locations. Left: Spectrum at FP-POS=1. Middle: Spectrum at FP-POS=4 shifted in pixel space so that an absorption feature overlaps. Right: Ratio of the two showing vignetting profile.

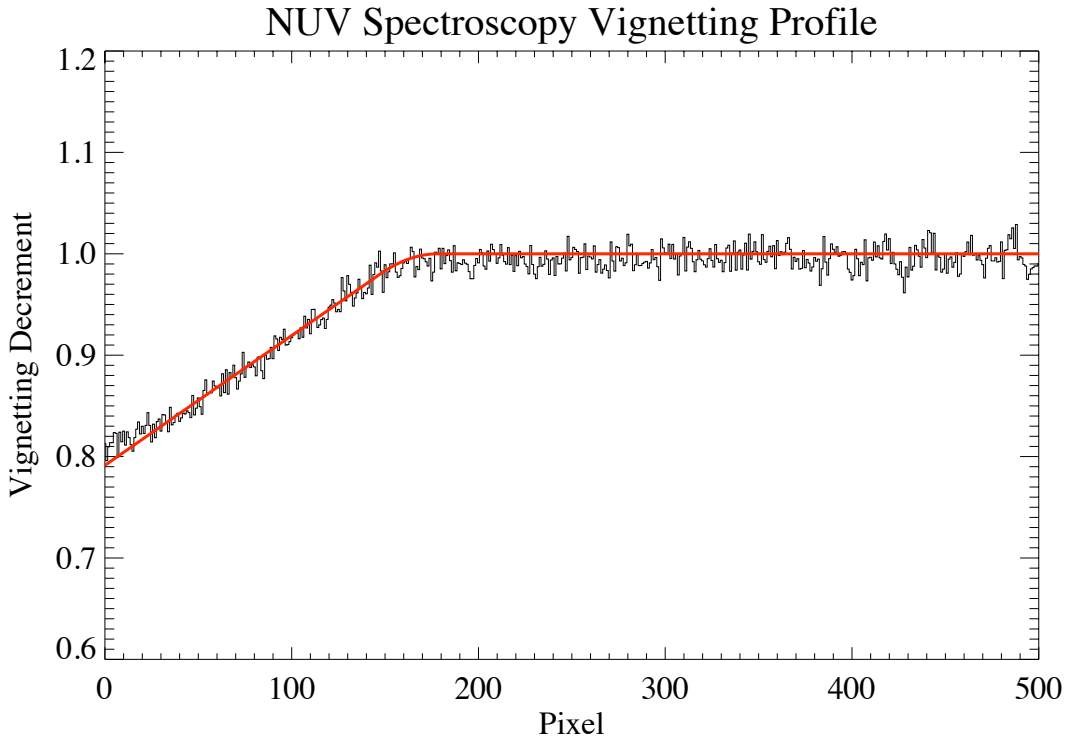

Figure 6: The final fit to the average of spectral ratios for the vignetting profile.

There is some indication that the vignetting profile is wavelength dependent, but this has yet to be explored more fully. The fit from the average profile does have systematic

differences for each of the individual spectral ratios; however for the M gratings, these are limited to about ±2.5%. The difference is greater for the G230L, with systematic offsets between 3-6%, though these spectra are noisier. We believe this is due to the difference in optical angles at which the G230L operates. A separate vignetting profile was fit for the G230L data that reduces the residual to a value consistent with those of the M gratings.

The most expedient method to make vignetting corrections in the CalCOS pipeline for Cycle 17 was to modify the NUV flat field reference file. Since the flat field is divided into the science data, the product of the P-flat with the vignetting profile generates a combined reference file that removes the depression. Two flat-field files were created, one for G230L observations, the other for those made with a medium resolution grating. A correction technique separate from the flat-fielding step in CalCOS is expected to be developed in the future.

5. Determination of S/N Capabilities

5.1 High S/N observations (Program 11481)

SMOV program 11481 observed G191-B2B with at least two different central wavelength settings in all three M gratings and at all four FP-POS settings. GD71 was observed for two settings of the G230L grating and all four FP-POS settings. Exposure times were chosen so that a S/N greater than 30 per resolution element would be achieved in all settings and a S/N greater than 100 per resolution element could be demonstrated for at least one setting.

5.2 Analysis

For each grating setting the data were analyzed in the following manner. The CalCOS pipeline was run using the superflat including the vignetting correction. For each stripe, spectra from the x1d files were co-added for all FP-POS settings. A line-free region of the resultant spectrum was chosen, being sure to include only those wavelengths sampled by all four FP-POS settings. This was fitted by a polynomial (usually order < 3 sufficed), and normalized by that polynomial. The inverse of the standard deviation of the normalized spectrum is the S/N for that spectrum. This was performed at 1, 2 and 3 pixel binnings. Figure 7 shows an example of the technique.

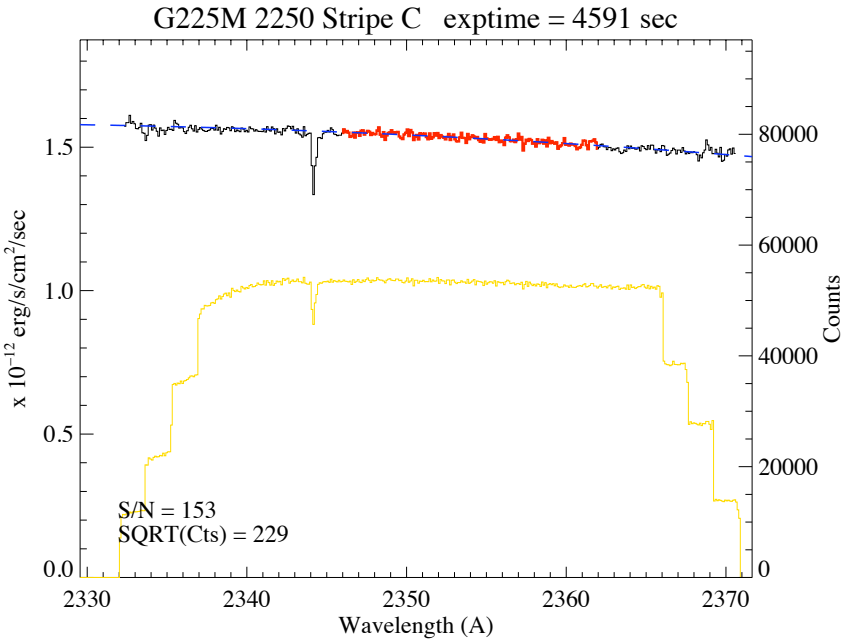

Figure 7: Co-added spectrum, binned by 3 pixels, of G191-B2B for one stripe of one NUV grating setting. The red region is the fitted region (dashed blue-line is best fit) while the yellow shows the counts spectrum.

5.3 S/N Versus Photon Statistics

The mesured S/N was compared to the Poisson limit of the observations (i.e., the square root of the counts), as shown in Figure 8. In all but two cases (Stripe C in the G230L data, which registers second order light), the resultant S/N was greater than 30 per 3 pixel resolution element, and several spectra had S/N>100. The achievable S/N can be represented by a function of the form, $(S/N_{actual})^{-2} = counts^{-1} + (S/N_{limit})^{-2}$. That equation is overplotted as a thick dashed line in Figure 8, with a S/N_{limit} of 231. The same fit was performed for the data without co-adding the various FP-POS spectra. The limiting S/N for an individual spectrum was thus determined to be about 115, shown as a thin dashed line in Figure 8. This is much higher than the maximum S/N ~ 30 obtainable without flat fielding. The combination of flat fielding and FP-POS summing recovers spectra to Poisson statistics up to S/N ~ 70 per resel. Above that, the achieveable S/N continues to improve, but does not reach the Poisson limit, most likely due to limitations in the flat-fielding process.

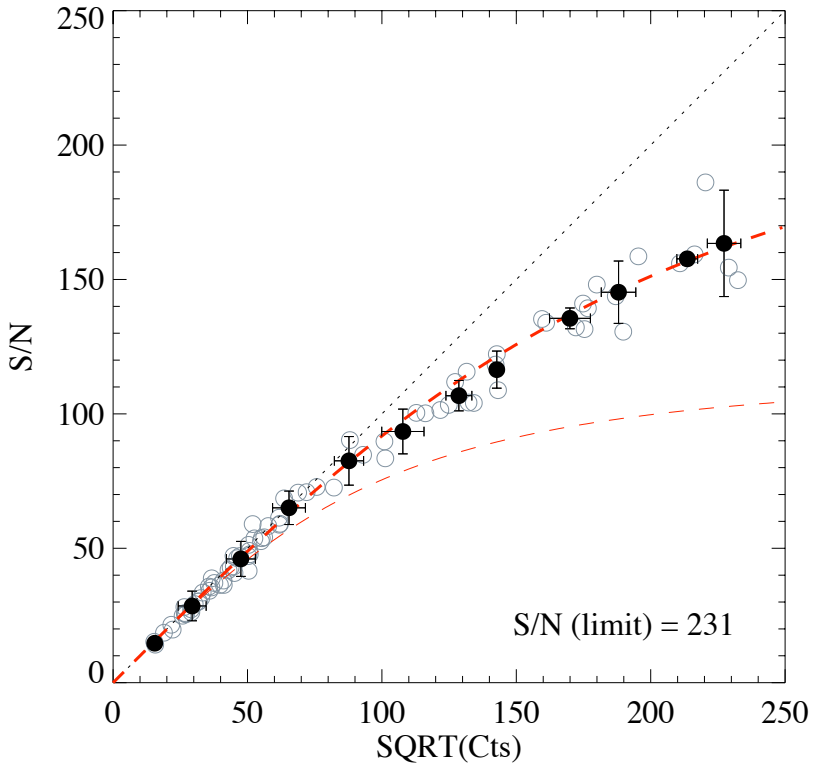

Figure 8: S/N achieved versus square root of the counts per resel. Each solid point is the average of multiple points (open gray circles). The dotted line across the diagonal is the Poisson limit. The best fit limiting S/N curve is shown as a thick dashed red line. The thin dashed red line is the best fit for the data that was not co-added from the FP-POS spectra.

6. Summary

We have analyzed the COS NUV flat-field data taken during SMOV and find that the on-orbit flat field aligns within one pixel of the flat field created during TV testing. All SMOV and TV data were then combined to produce a superflat reference file to be used in pipeline processing. The reference file includes a correction for vignetting at lower X pixel values of the MAMA, which is not present in the flat-field data but is seen in exposures of external targets. Studies of the S/N achievable with flat fielding and FP-POS stepping indicates that the Poisson limit can be reached for S/N < 70. S/N > 150 was demonstrated for the SMOV high S/N program.

7. Change History for COS ISR 2010-03

Version 1: 04 February 2010 - Original Document

8. References

COS AV-04, “COS Prelaunch Calibration Data”, 2004

COS OP-01, “Cosmic Origins Spectrograph (COS) Science Operations Requirements Document”, 2003

Soderblom, D. R. et al 2007, “Cosmic Origins Spectrograph Instrument Handbook”, version 1.0, (Baltimore, STScI)